Electronic Supplementary Information

A methylation-switchable conformational probe for sensitive and selective detection of RNA demethylase activity†

Tianming Yang,‡ Adeline Cheong,‡ Xiangrui Mai, Shui Zou and Esther C. Y. Woon*

Department of Pharmacy, National University of Singapore, 18 Science Drive 4, 117543, Singapore.

‡ These authors contributed equally to the work.

* To whom correspondence should be addressed.

Esther C. Y. Woon

Email: esther.woon@nus.edu.sg Fax: Tel: (+65) 6516 2932; (+65) 6779 1554. Address: Department of Pharmacy, National University of Singapore, 18 Science Drive 4, 117543, Singapore.

Contents:

Table S1. Preliminary assessment on the suitability of several RNA (**1-10**) and DNA (**11-14**) sequences as conformational probes. The red and blue letters indicate m^1A base in RNA and DNA, respectively. The sequences investigated are all based on Dickerson-Drew palindromic sequence. The melting temperatures (T_m) of the sequences were determined by DSF-based melting analysis (at 5 μM strand concentration in 10 mM sodium phosphate buffer, pH 7.0 containing 150 mM NaCl). CD analysis provides a qualitative picture of the conformational influence of m^1A methylation.

No.	length	Sequence	DSF melt profile	T_m (°C) (at 5 μM)	ΔT_m (°C)*	Conformation (CD analysis)
1	12mer	r(CGCGAUAUCGCG)	monophasic	63.9	5.9	A-form duplex
2		r(CGCG**A**UAUCGCG)	monophasic	69.8		B-like hairpin
3 (Demethylated probe)	12mer	r(CGCGAAUUCGCG)	monophasic	62.3	6.4	A-form duplex
4 (m^1A-probe)		r(CGCG**A**AUUCGCG)	monophasic	68.7		B-like hairpin
5	14mer	r(CGCGCAAUUGCGCG)	monophasic	67.2	6.7	A-form duplex
6		r(CGCGC**A**AUUGCGCG)	monophasic	73.9		B-like hairpin
7	16mer	r(CGCGCGAAUUCGCGCG)	monophasic	72.5	--	A-form duplex
8		r(CGCGCG**A**AUUCGCGCG)	biphasic	80.1; 89.7		B-like hairpin
9	20mer	r(CGCGCGCGAAUUCGCGCGCG)	monophasic	81.0	--	A-form duplex
10		r(CGCGCGCG**A**AUUCGCGCGCG)	--	>95		mixture
11	12mer	d(CGCGAATTCGCG)	biphasic	45.3; 68.6	--	mixture
12		d(CGCG**A**ATTCGCG)	monophasic	58.3		B-form duplex
13	12mer	d(CGCGATATCGCG)	biphasic	42.1; 71.3	--	mixture
14		d(CGCG**A**TATCGCG)	monophasic	72.5		B-form duplex

* Difference in T_m between the methylated and unmethylated sequences.

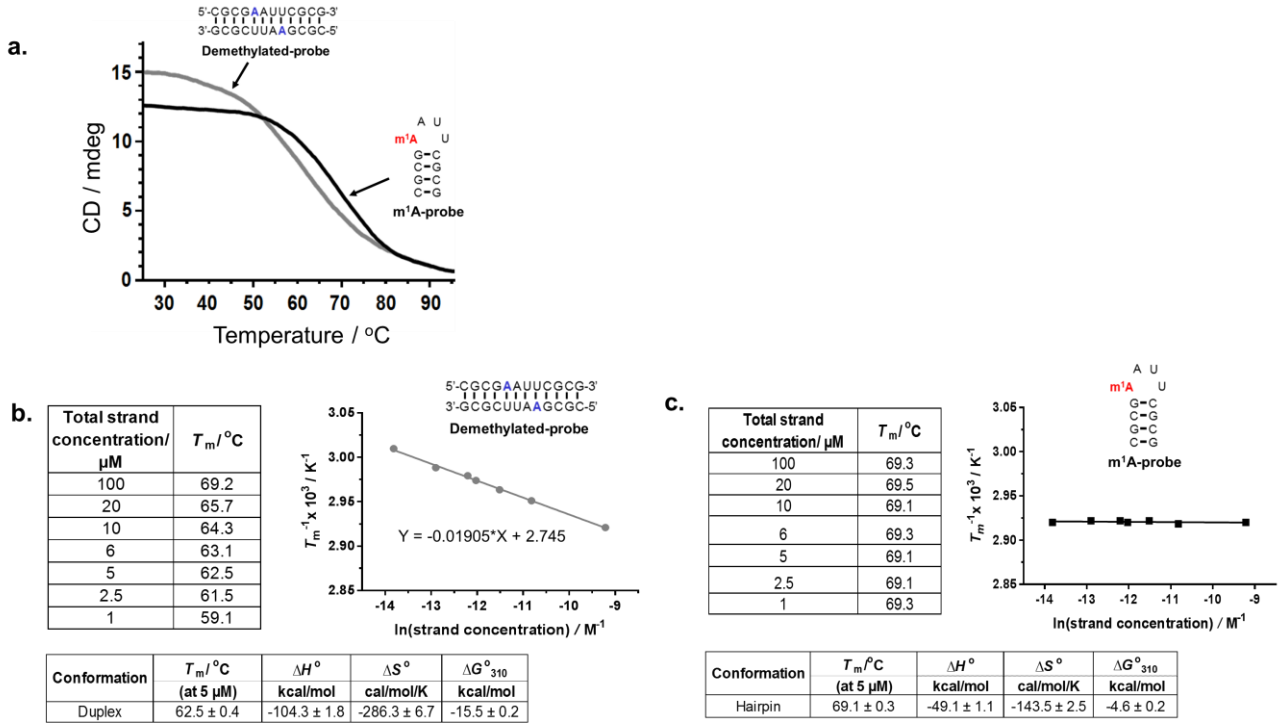

Figure S1. CD-based melting analysis of m^{1}A- and demethylated probes. (a) Overlay of the CD melting profile of m^{1}A-probe (black line) and demethylated-probe (grey line), both measured at 5 µM total strand concentrations in 10 mM sodium phosphate buffer containing 150 mM NaCl, pH 7.0. The melt profile revealed a monophasic, sigmoid melt transition, implying that both probes exist predominantly as single conformation under our experimental conditions. (b) Van't Hoff analysis of the demethylated probe revealed concentration-dependent T_m, implying a bimolecular duplex structure. The thermodynamic data were derived from $1/T_m$ versus ln(strand concentration) plot, assuming a two-state process. (c) Van't Hoff plot of m^{1}A-probe at concentrations between 1-100 µM showed concentration-independent T_m (69.1 °C), implying the presence of a monomolecular hairpin structure. The thermodynamic data were obtained from α (the fraction of strands remaining hybridised) versus temperature plot by curve fitting to a two-state transition model. The melt transitions obtained from CD analysis are highly consistent with those derived from UV- and DSF-melting analyses (Fig. S2-S4).

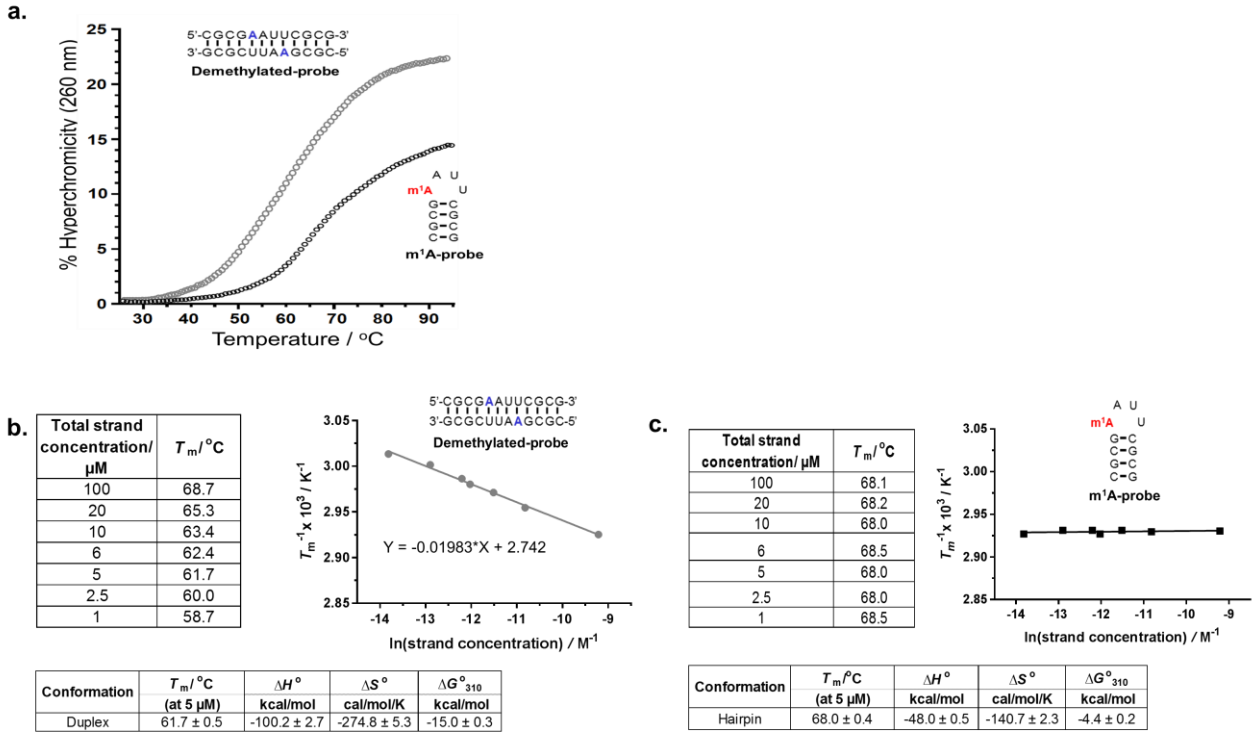

Figure S2. UV-based melting analysis of m^{1}A- and demethylated probes. (a) Overlay of the UV melting profile of m^{1}A-probe (black line) and demethylated-probe (grey line), both measured at 5 µM total strand concentrations in 10 mM sodium phosphate buffer containing 150 mM NaCl, pH 7.0. The melt profile revealed a monophasic, sigmoid melt transition, implying that both probes exist predominantly as single conformation under our experimental conditions. (b) Van't Hoff analysis of the demethylated probe revealed concentration-dependent T_m, implying a bimolecular duplex structure. The thermodynamic data were derived from $1/T_m$ versus ln(strand concentration) plot, assuming a two-state process. (c) Van't Hoff plot of m^{1}A-probe at concentrations between 1-100 µM showed concentration-independent T_m (68.0 °C), implying the presence of a monomolecular hairpin structure. The thermodynamic data were obtained from α (the fraction of strands remaining hybridised) versus temperature plot by curve fitting to a two-state transition model. The melt transitions obtained from UV analysis are highly consistent with those derived from CD- and DSF-melting analyses (Fig. S1, S3 and S4).

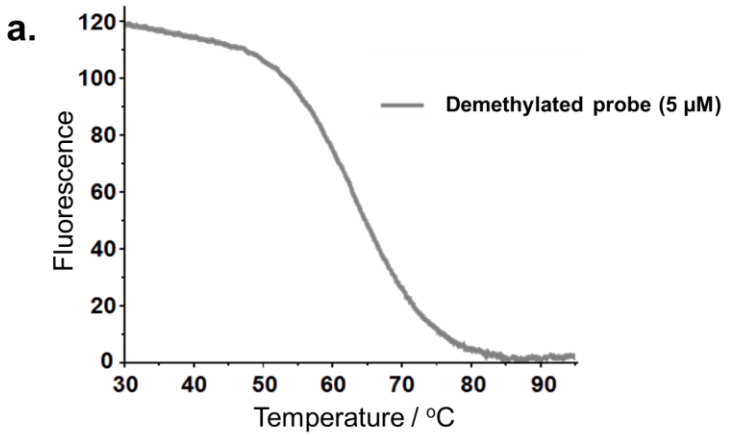

b.

Total strand concentration/ µM	T_m/°C
100	68.8
20	65.4
10	63.5
6	63.0
5	62.3
2.5	61.1
1	59.2

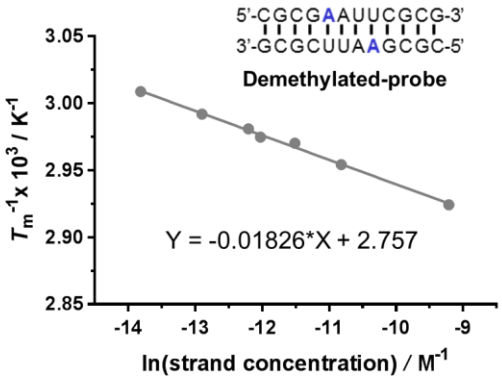

Conformation	T_m/°C (at 5 µM)	$\Delta H°$ kcal/mol	$\Delta S°$ cal/mol/K	$\Delta G°_{310}$ kcal/mol
Duplex	62.3 ± 0.2	-108.8 ± 1.2	-300.0 ± 3.4	-15.8 ± 0.2

Figure S3. DSF-based melting analysis of the demethylated-probe. (a) Fluorescence spectrum of demethylated-probe at 5 µM total strand concentrations in 10 mM sodium phosphate buffer containing 150 mM NaCl, pH 7.0. The melt profile revealed a monophasic, sigmoid melt transition, implying that the probe exist predominantly as a single conformation under our experimental conditions. (b) Van't Hoff plot at concentrations between 1-100 µM showed dependence of melting temperatures on strand concentrations, implying a bimolecular duplex structure. The thermodynamic data were derived from $1/T_m$ versus ln(strand concentration) plot, assuming a two-state process.

a.

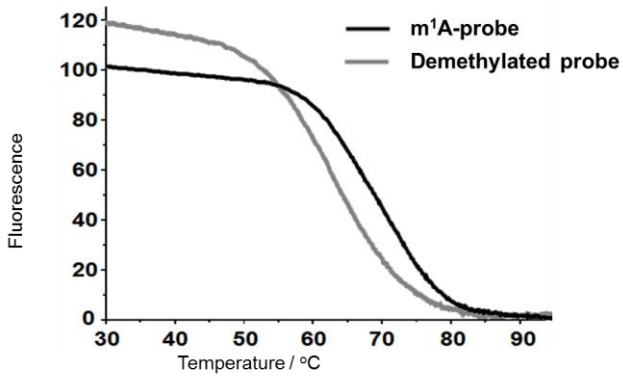

b.

Total strand concentration/ µM	T_m / °C
100	68.9
20	68.5
10	68.6
6	68.5
5	68.7
2.5	68.7
1	68.8

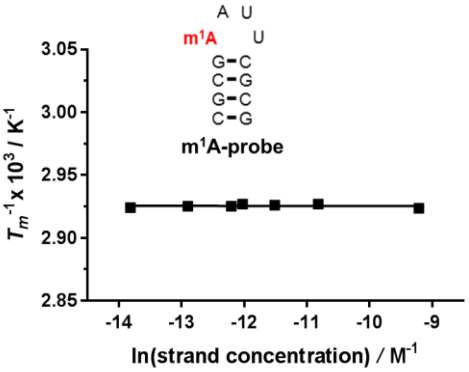

Conformation	T_m/°C (at 5 µM)	$\Delta H°$ kcal/mol	$\Delta S°$ cal/mol/K	$\Delta G°_{310}$ kcal/mol
Hairpin	68.7 ± 0.3	-46.9 ± 0.9	-137.0 ± 2.1	-4.3 ± 0.1

Figure S4. DSF-based melting analysis of the m^{1}A-probe. (a) Overlay of the fluorescence spectra of m^{1}A-probe (black line) and demethylated-probe (grey line), both measured at 5 µM total strand concentrations in 10 mM sodium phosphate buffer containing 150 mM NaCl, pH 7.0. The melt profile of m^{1}A-probe revealed a monophasic, sigmoid melt transition, implying that the probe exist predominantly as a single conformation under our experimental conditions. There is a large change in T_m between m^{1}A-probe and its demethylated equivalent (ΔT_m = 6.4 °C). (b) Van't Hoff plot of m^{1}A-probe at concentrations between 1-100 µM showed concentration-independent T_m (68.7 °C), implying the presence of a monomolecular hairpin structure. The thermodynamic data were obtained from α (the fraction of strands remaining hybridised) versus temperature plot by curve fitting to a two-state transition model.

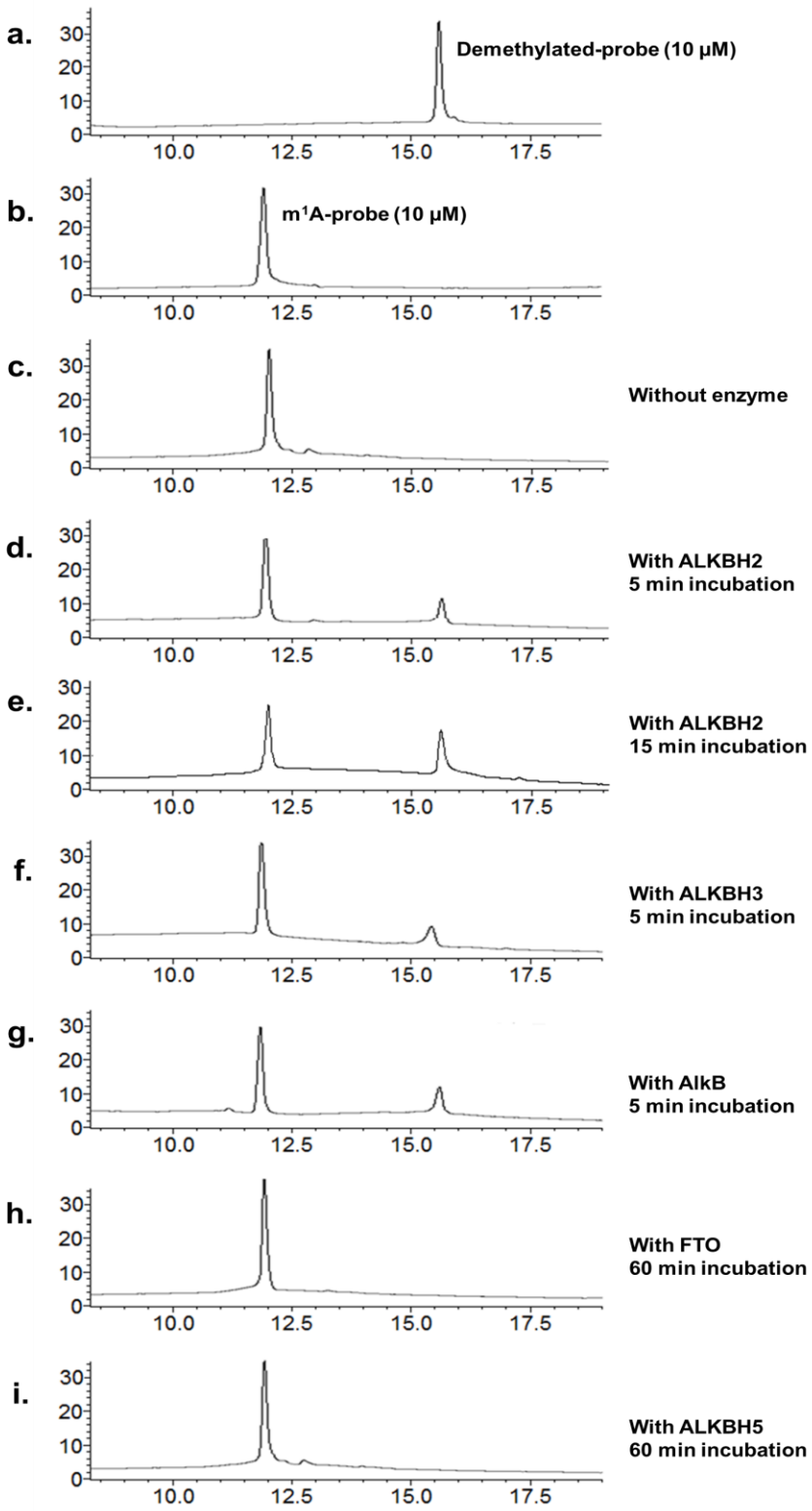

Figure S5. Analysis of m^1A-probe demethylation by AlkB demethylases with HPLC-based assay. Reaction consisted of the enzyme (0.1 μM), m^1A-probe substrate (10 μM), 2-oxoglutarate (150 μM), $(NH_4)_2Fe(SO_4)_2 \cdot 6H_2O$ (150 μM), and L-ascorbate (2 mM) in 50 mM

HEPES buffer, pH 7.0. Consistent with demethylation-induced conformational change, standard preparations of (a) demethylated-probe product (10 μM; Rt = 15.6 min; duplex) eluted with considerably longer retention time than (b) m^1A-probe substrate (10 μM; Rt = 11.9 min; hairpin). Hence, the conformational probe approach could also facilitate the analysis of demethylase activity by HPLC-based methods. Representative HPLC traces of reaction mixtures (c) in the absence of enzyme (control), and after treatment with (d,e) ALKBH2, (f) ALKBH3, and (g) AlkB. The m^1A-probe substrate was found to be efficiently demethylated by all m^1A demethylases investigated, with demethylation yields of approximately 15% after a 5-min incubation. (e) There was an increased formation of demethylated product (40% yield), coupled with a corresponding decrease in substrate after 15 min incubation with ALKBH2. The m^1A-probe was also found to be highly selectivity for m^1A demethylases, as demonstrated by the lack of product formation with (h) FTO and (i) ALKBH5, even after prolonged (1 hour) incubation.

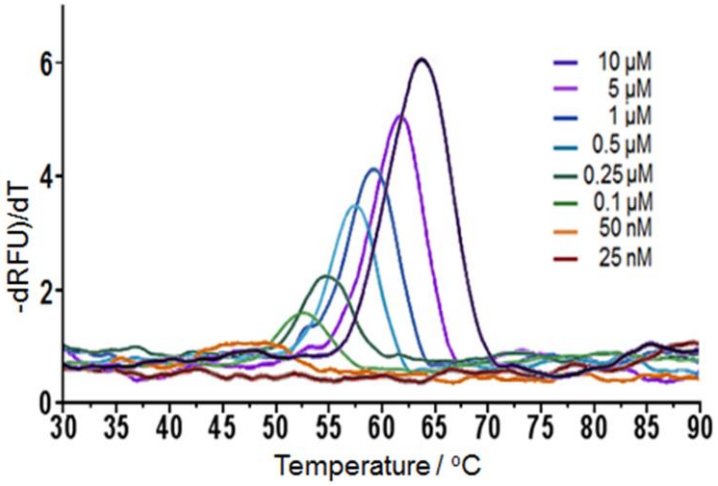

Figure S6. DSF sensitivity tests. The melting profiles of reaction mixtures contained varying concentrations of demethylated-probe (25 nM -10 µM) and 20x SYBR Green I were obtained by steady heating from 25 °C to 95 °C at a rate of 1 °C / min-1. Fluorescence were detected on FAM channel, with readings taken every 0.5 °C. The software provided was then used to normalise the fluorescence spectra, and to obtain the negative first derivative plots. The results show that DSF-base melting analysis has the sensitivity to reliably detect serially diluted product as little as 100 nM.

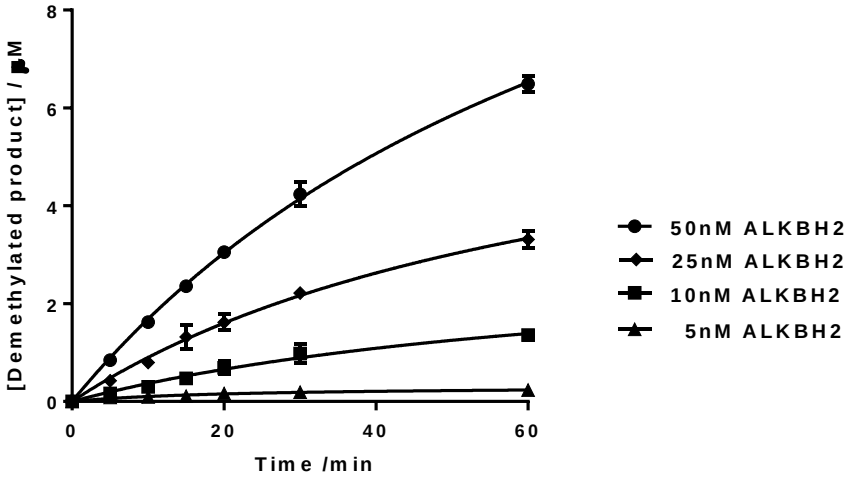

Figure S7. Enzyme titration studies. The conformational probe-DSF assay was run at different ALKBH2 concentrations for various time intervals (5, 10, 15, 20, 30 and 10 minute) at 4 ºC. The reaction was then quenched and monitored for product formation by DSF-melting analysis. The time courses over 60 min show that demethylase activity can be measured at ALKBH2 concentrations as low as 10 nM, with the initial rates being proportional to enzyme concentrations. All assays were performed in 50 mM HEPES buffer (pH 7.0) containing m^1A-probe substrate (10 µM), 2-oxoglutarate (10 µM), (NH4)2Fe(SO4)2·6H2O (10 µM), and L-ascorbate (200 µM). Errors represent S.D. of three replicates.

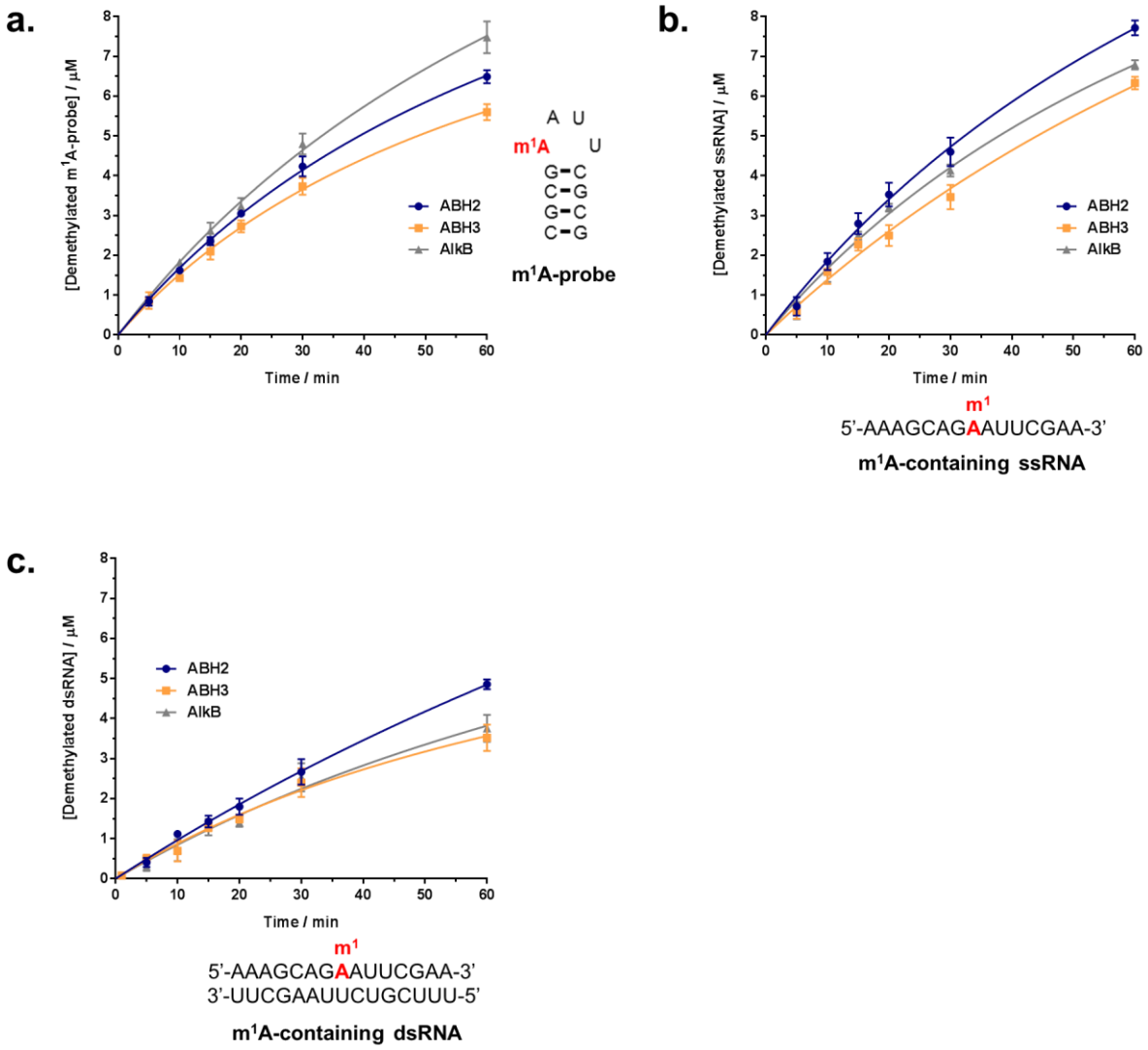

Figure S8. Time course analysis of the demethylation of (a) m1A-probe, (b) m^1A-containing ssRNA, and (c) m^1A-containing dsRNA by m^1A demethylases (ALKBH2, ALKBH3 and AlkB). The concentration of demethylated product at different substrate concentrations was plotted as a function of time. All reactions were performed at 4 ^oC, pH 7.0. Errors represent S.D. of three replicates.

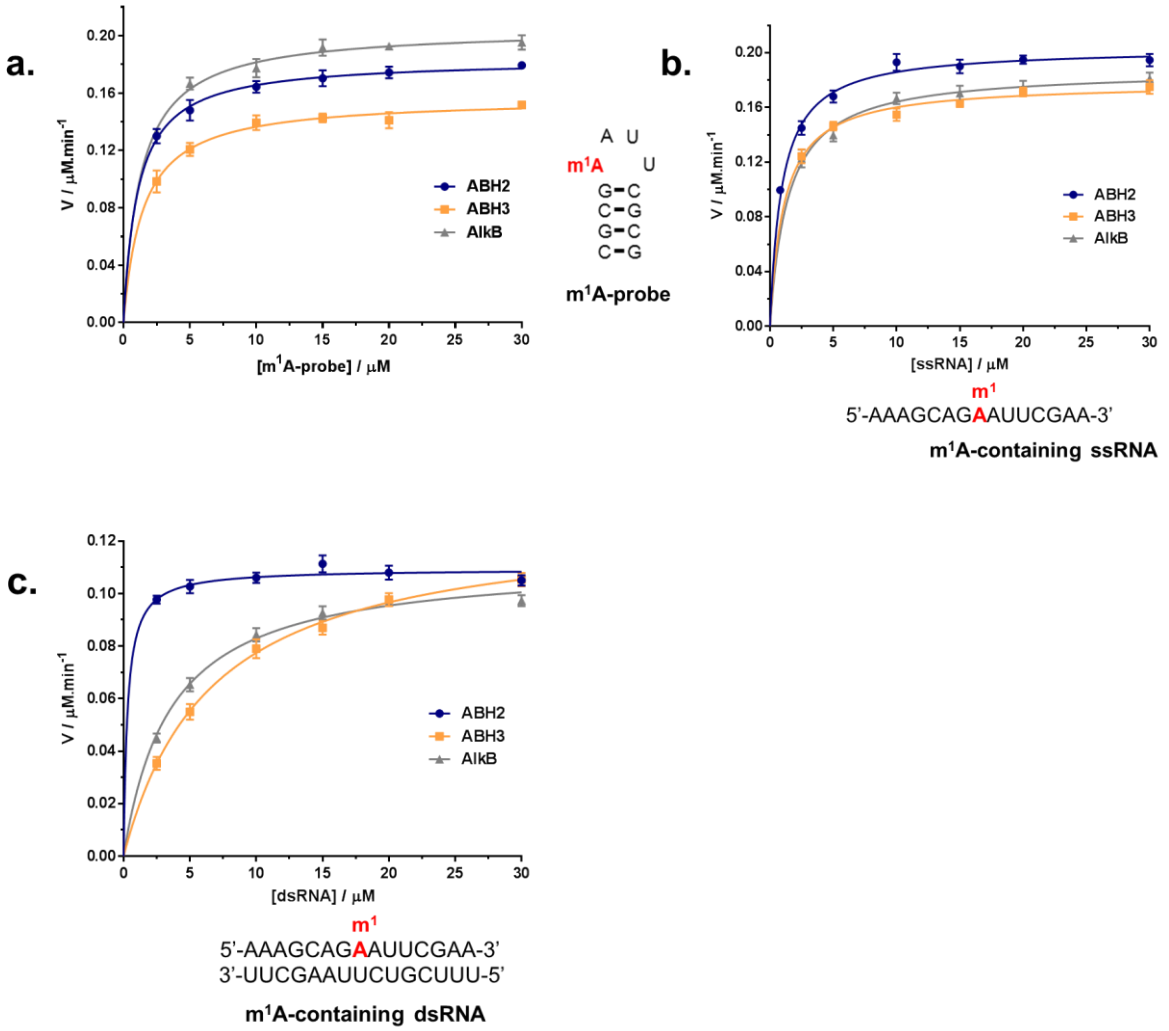

Figure S9. Steady-state kinetics analyses of the demethylation of (a) m1A-probe, (b) m^1A-containing ssRNA, and (c) m^1A-containing dsRNA by m^1A demethylases (ALKBH2, ALKBH3 and AlkB). The K_m and k_{cat} values were determined by keeping a constant enzyme concentration of 50 nM and varying the substrate concentrations (2.5, 5, 10, 15, 20 and 30 μM). All reactions were performed at 4 ºC in triplicate and were adjusted to ensure that less than 20% of the substrate was consumed. Errors represent S.D. of three replicates.

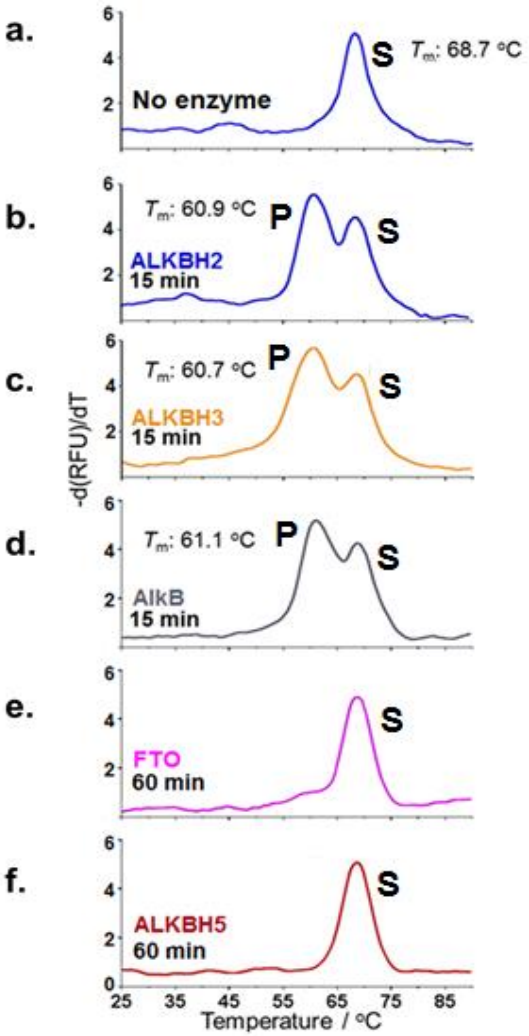

Figure S10. Analysis of m^1A-probe demethylation by AlkB demethylases with DSF-based assay. The enzyme (50 nM) was incubated with m^1A-probe (10 µM) in the presence of 2-oxoglutarate (10 µM), Fe(II) (10 µM), and L-ascorbate (200 µM) in 50mM HEPES buffer (pH 7.0) at 4 °C. SYBR Green I (20x) was then added and the mixture monitored for product formation using DSF-melting analysis. The negative first derivative plots show melting profiles of reaction mixtures (a) in the absence of enzyme, and after 15 minute incubation with (b) ALKBH2, (c) ALKBH3 and (d) AlkB, where a distinct biphasic melt transitions were observed, indicating conversion of m^1A-probe to demethylated-probe. The observed demethylation reaction was specifically catalysed by m^1A demethylases, as demonstrated by the lack of product formation when m^1A-probe was incubated with structurally-related AlkB subfamily members (e) ALKBH5, and (f) FTO, both of which are specific for m^6A, with negligible activity towards m^1A substrates. An omission of any of the assay components (Fe(II), 2OG) also gave no demethylation product (results not shown).S and P denotes melt transitions for m^1A-probe substrate and demethylated-probe product, respectively.

a.

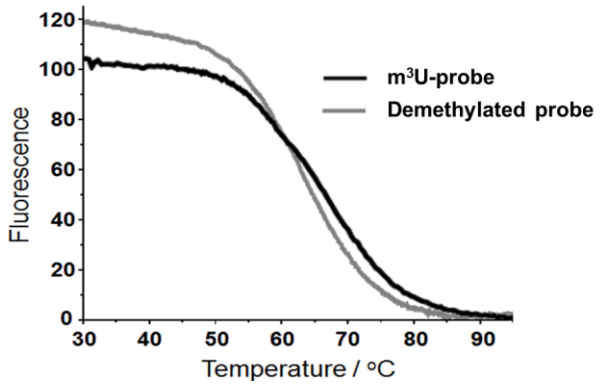

b.

Total strand concentration/ µM	T_m/°C
100	66.3
20	66.5
10	66.8
6	66.2
5	66.5
2.5	66.4
1	66.7

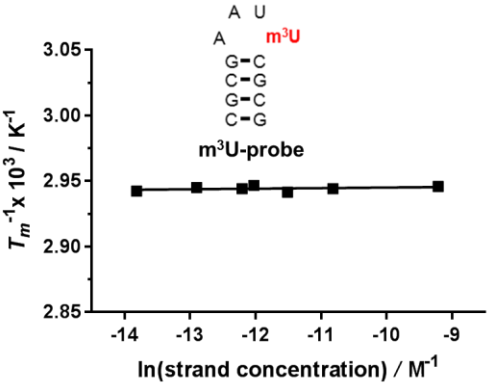

Conformation	T_m/°C (at 5 µM)	$\Delta H°$ kcal/mol	$\Delta S°$ cal/mol/K	$\Delta G°_{310}$ kcal/mol
Hairpin	66.5 ± 0.2	-44.3 ± 0.7	-130.4 ± 1.7	-3.8 ± 0.2

Figure S11. DSF-based melting analysis of the m^{3}U-probe. (a) Overlay of the fluorescence spectra of m^{3}U-probe (black line) and demethylated-probe (grey line), both measured at 5 µM total strand concentrations in 10 mM sodium phosphate buffer containing 150 mM NaCl, pH 7.0. The melt profile of m^{3}U-probe revealed a monophasic, sigmoid melt transition, implying that the probe exist predominantly as a single conformation under our experimental conditions. There is significant change in T_m between m^{3}U-probe and its demethylated equivalent (ΔT_m = 4.2 °C). (b) Van't Hoff plot of m^{3}U-probe at concentrations between 1-100 µM showed concentration-independent T_m (66.5 °C), implying the presence of a monomolecular hairpin structure. The thermodynamic data were obtained from α (the fraction of strands remaining hybridised) versus temperature plot by curve fitting to a two-state transition model.

a.

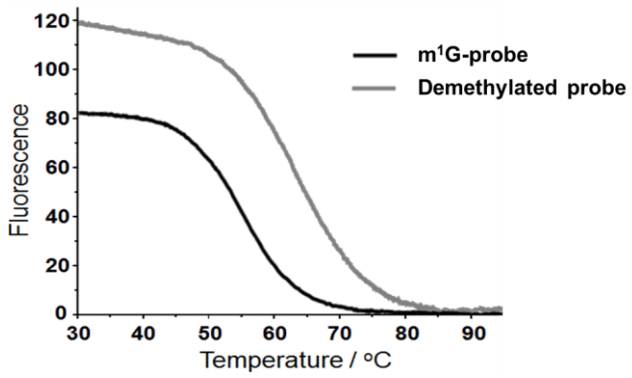

b.

Total strand concentration/ μM	T_m/°C
100	54.2
20	54.9
10	54.3
6	54.8
5	54.6
2.5	54.2
1	54.8

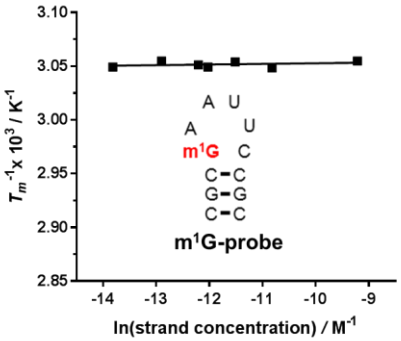

Conformation	T_m/°C (at 5 μM)	$\Delta H°$ kcal/mol	$\Delta S°$ cal/mol/K	$\Delta G°_{310}$ kcal/mol
Hairpin	54.6 ± 0.3	-36.8 ± 1.5	-112.3 ± 3.6	-2.0 ± 0.1

Figure S12. DSF-based melting analysis of the m^{1}G-probe. (a) Overlay of the fluorescence spectra of m^{1}G-probe (black line) and demethylated-probe (grey line), both measured at 5 μM total strand concentrations in 10 mM sodium phosphate buffer containing 150 mM NaCl, pH 7.0. The melt profile of m^{1}G-probe revealed a monophasic, sigmoid melt transition, implying that the probe exist predominantly as a single conformation under our experimental conditions. There is a large change in T_m between m^{1}G-probe and its demethylated equivalent (ΔT_m = 7.7 °C). (b) Van't Hoff plot of m^{1}G-probe at concentrations between 1-100 μM showed concentration-independent T_m (54.6 °C), implying the presence of a monomolecular hairpin structure. The thermodynamic data were obtained from α (the fraction of strands remaining hybridised) versus temperature plot by curve fitting to a two-state transition model.

a.

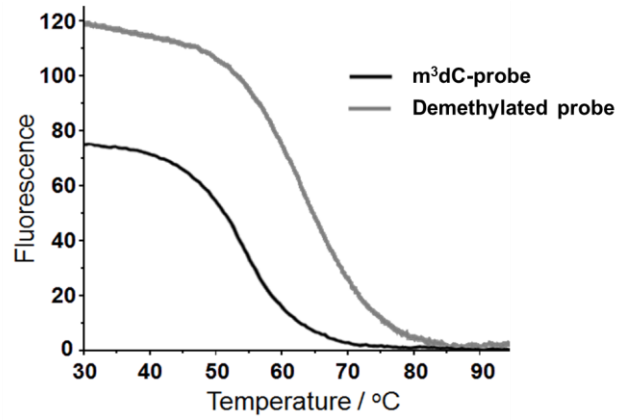

b.

Total strand concentration/ µM	T_m / °C
100	54.0
20	54.2
10	53.7
6	53.5
5	53.9
2.5	54.1
1	53.9

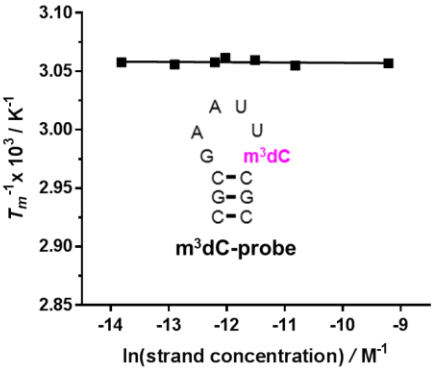

Conformation	T_m/°C (at 5 µM)	$\Delta H°$ kcal/mol	$\Delta S°$ cal/mol/K	$\Delta G°_{310}$ kcal/mol
Hairpin	53.9 ± 0.1	-34.7 ± 1.3	-106.1 ± 2.1	-1.8 ± 0.1

Figure S13. DSF-based melting analysis of the m^{3}dC-probe. (a) Overlay of the fluorescence spectra of m^{3}dC-probe (black line) and demethylated-probe (grey line), both measured at 5 µM total strand concentrations in 10 mM sodium phosphate buffer containing 150 mM NaCl, pH 7.0. The melt profile of m^{3}dC-probe revealed a monophasic, sigmoid melt transition, implying that the probe exist predominantly as a single conformation under our experimental conditions. There is a large change in T_m between m^{3}dC-probe and its demethylated equivalent (ΔT_m = 8.4 °C). (b) Van't Hoff plot of m^{3}dC-probe at concentrations between 1-100 µM showed concentration-independent T_m (53.9 °C), implying the presence of a monomolecular hairpin structure. The thermodynamic data were obtained from α (the fraction of strands remaining hybridised) versus temperature plot by curve fitting to a two-state transition model.

Materials and Methods

Synthesis and purification of the conformational probes

The RNA conformational probes used in this study were synthesised using standard β-cyanoethyl phosphoramidite chemistry, and adapted form previously reported procedures.[1] All synthesiser reagents and phosphoramidites were purchased from Glen Research. In brief, the oligonucleotides were synthesised on a solid support by the automated DNA/RNA synthesiser (Applied Biosystems 394) using a standard 1.0 µmole phosphoramidite cycle of acid-catalysed detritylation, coupling, capping, and iodine oxidation. Coupling of the modified monomer was allowed to proceed for 10 min. Cleavage of the oligonucleotides from the solid support and deprotection was achieved by treatment with an anhydrous solution of 2 M ammonia in MeOH for 60 h at room temperature. Mild coupling and deprotection approach was employed to avoid potential Dimroth rearrangement of m^1A (to m^6A) under basic conditions.[2] The crude products were purified by reverse-phase HPLC using the Waters XBridge OST C18 column (2.5 micron, 10 mm × 50 mm). HPLC solvents used were: solvent A (100 mM triethylammonium acetate buffer, pH 6.5 with 5% acetonitrile) and solvent B (100 mM triethylammonium acetate buffer, pH 6.5 with 15% acetonitrile) with a flow rate of 5 mL/ min. All purified oligonucleotides were characterized by MALDI-MS and capillary gel electrophoresis, and were found to be at least 95% pure. The MALDI-MS data for all RNA probes investigated in this study are summarised in the table below.

No.	Sequence	MALDI-MS	
		$[M+H]^+$ (calculated)	$[M+H]^+$ (observed)
Demethylated-probe	r(CGCGAAUUCGCG)	3811.4	3811.2
m^1A-probe	r(CGCG**m^1A**AUUCGCG)	3826.4	3826.3
m^3U-probe	r(CGCGAAU**m^3U**CGCG)	3825.4	3825.5
m^1G-probe	r(CGC**m^1G**AAUUCGCG)	3825.4	3825.1
m^3dC-probe	r(CGCGAAUU**m^3dC**GCG)	3810.4	3810.6

Differential Scanning Fluorimetry (DSF)-based melting analysis

DSF-based melting analysis was performed using a CFX96 Real-Time PCR Detection System (Bio-Rad). The reaction mixture contained varying concentrations of RNA probe (1-100 μM) and 20x SYBR Green I (Invitrogen; a duplex-intercalating fluorescent dye) in a final volume of 50 μl. Melting curve was obtained by steady heating from 25 °C to 95 °C at a rate of 1 °C / min^{-1}. Fluorescence were detected on FAM channel, with readings taken every 0.5 °C. The software provided was then used to normalise the fluorescence spectra, and to obtain the negative first derivative plots, from which the T_m is determined.

For sample preparation, the lyophilised RNA probes were reconstituted in 10 mM sodium phosphate buffer (pH 7.0) solution containing 150 mM NaCl. Their concentrations were determined by UV absorbance at 260 nm (A_{260}) using a NanoDrop ND-1000 UV-Visible Spectrophotometer. Extinction coefficients were calculated using the nearest neighbour approximation; the extinction coefficients of RNAs containing methylated bases were assumed to be the same as those containing unmodified bases. Each probe was measured at seven different concentrations (1, 2.5, 5, 6, 10, 20 and 100 μM), and a total of six melting transitions were measured for each RNA probe concentration. Melting transitions were generally found to be reproducible for all probes.

Analysis of thermodynamic data from DSF-melting experiments

The thermodynamic data for bimolecular duplex structure *i.e.* the demethylated-probe was analysed as previously described, with modifications.[3] The melting transitions for duplex structures were assumed to proceed in a two-state manner, and to obey the van't Hoff's equation below.

$$\frac{1}{T_m} = \frac{R}{\Delta_b H^\circ} \ln c_T + \frac{\Delta_b S^\circ}{\Delta_b H^\circ}$$

A plot of $1/T_m$ versus ln(total strand concentration) gives a straight line, where the slope is $R/\Delta H°$ and the y-intercept is $\Delta S°/\Delta H°$. Data were fitted using linear least-squares minimisation using GraphPad Prism. The free Gibbs energy ($\Delta G°$) were calculated at 37 °C (310.15 K) using the following equation.

$$\Delta_b G^\circ = \Delta_b H^\circ - T\Delta_b S^\circ$$

The thermodynamic data for monomolecular hairpin structures *i.e.* m^1A-, m^3U, m^1G and m^3dC-probes was analysed as previously described, with modifications.[4] The experimental fluorescence versus temperature curves were first converted into a fraction of strands remaining hybridized (α) versus temperature curves. This were then fitted to a two-state transition model, where $\Delta H°$ and $\Delta S°$ values may be obtained.

Circular dichroism (CD) spectroscopy of the conformational probes

The CD spectra for the m^1A-probe and demethylated-probe were obtained with a JASCO J-810 spectropolarimeter. The measurements were carried out with 5 μM probes in a 10 mM sodium phosphate buffer (pH 7.0) containing 150 mM NaCl at 25 °C. The concentrations were determined by UV absorbance at 260 nm (A_{260}) using a NanoDrop ND-1000 UV-Visible Spectrophotometer. The probe solutions were first heated to 90 °C for 5 min, and re-annealed by slow cooling to 4 °C at a rate of 1 °C/min. CD spectra were then recorded in quartz cuvettes (path length 1 mm, 400 μL) from 200 nm to 350 nm at 4 °C using a 10 nm/min scan speed, a spectral band width of 1 nm and a time constant of 4 s. All the spectra were subtracted with the buffer blank and smoothed using the Savitsky-Golay algorithm (polynomial order 10).

CD-based melting analysis

The CD melting curves were performed by measuring the absorptivity at a single wavelength, 260 nm for demethylated probe and 270 nm for m^1A-probe, with a temperature range of 25 °C to 95 °C and a temperature slope of 1°C/min. The samples were measured at a concentration of 5 μM probes in 10 mM sodium phosphate buffer (pH 7.0) containing 150 mM NaCl. The melting point T_m, the enthalpy $\Delta H°$ and entropy $\Delta S°$ were determined using curve fitting analyses similar to that described for DSF-melting experiments above.

UV-based melting analysis

The melting of each RNA probes was performed on a Cary 3000 UV-Visible Spectrophotometer (Varian) at a total strand concentration of 5 μM (unless stated otherwise) in 10 mM sodium phosphate buffer, pH 7.0 and 150 mM NaCl. Absorbance versus temperature profiles were recorded at 260 nm. The samples were first denatured by heating to 95 °C at 10 °C/min, followed by slow cooling to 25 °C at 0.4 °C/min to ensure a complete annealing of the strands. The melting transitions were then monitored by heating to 95 °C at 0.4 °C/min. To increase the accuracy of measurements, the sixth position was used to record the temperature data points by placing a temperature probe directly in the cuvette. Up to six melting transitions

were measured for each oligonucleotide and the average T_m values were calculated using Varian Cary Software.

^{1}H NMR spectroscopy of the conformational probes

All ^{1}H NMR experiments were performed on a Bruker DRX-500 spectrometer operating at 500.23 MHz. The imino spectra were acquired using water suppression by gradient-tailored excitation (WATERGATE) pulse sequence.[5] Both the m^{1}A-probe and demethylated-probe were measured at four different temperatures (25 °C, 15 °C, 4 °C and 1 °C), at concentrations of 1.2 mM and 0.3 mM, respectively. For sample preparation, the RNA probes were dissolved in a 9:1 buffer/ D_2O mix. The buffer used was 10 mM Na_2HPO_4 buffer, pH 7.0, containing 150 mM NaCl.

Human ALKBH2 expression and purification

Human ALKBH2 was expressed and purified as previously reported, with modifications.[6-8] A His_6-tagged $ALKBH2_{56-258}$ construct in pET28b was transformed into *E. coli* BL21 (DE3) Rosetta cells. The transformed cells were grown at 37 ^oC and 200 rpm to an OD_{600} of 0.6. ALKBH2 expression was induced by addition of 0.5 mM IPTG (Gold Biotechnology). Growth was continued at 37 ^oC for 4 h, after which the cells were harvested by centrifugation. The resulting cell pellet was stored at -80 ^oC. Cell pellets were resuspended to homogeneity in 50 mM Sodium Phosphate buffer, pH 8.0, containing 300 mM NaCl, 10% (v/v) glycerol and 5 mM β-ME. The cells were then disrupted by sonication on ice, and the cell lysate centrifuged and filtered. ALKBH2 was purified from the crude cell lysate by Ni affinity chromatography (GE healthcare), with elution achieved by application of gradient to 500 mM imidazole. This was followed by anion chromatography using a 5 mL HiTrap Q HP column (GE healthcare), with elution achieved by application of gradient to 1 M NaCl. Further purification was achieved by gel filtration using a HiLoad superdex 75 26/60 (GE healthcare) in a buffer of 10 mM Tris, pH 8.0, containing 100 mM NaCl and 5 mM β-ME. $ALKBH2_{56-258}$ has previously been shown to be catalytically active.[8]

Human ALKBH3 expression and purification

Full length human ALKBH3 was expressed and purified as previously reported, with modifications.[7,9] Full length human ALKBH3 was sub-cloned into pET28a to generate a His_6-tagged $ALKBH3_{1-286}$ construct, which was transformed into *E. coli* BL21 (DE3) Rosetta cells. The transformed cells were grown at 37 °C and 200 rpm until an OD_{600} of 0.6 was reached.

ALKBH3 expression was then induced by addition of 0.5 mM isopropyl β-D-1-thiogalactopyranoside (IPTG, Gold Biotechnology). Cell growth was continued at 37 °C for 4 h, after which the cells were harvested by centrifugation and the resulting cell pellet was stored at -80 °C. The frozen cell pellets were thawed and re-suspended to homogeneity in 50 mM Sodium Phosphate, pH 8.0, 300 mM NaCl, 10 mM imidazole and 5 mM β-ME. The cells were then disrupted by sonication on ice, and the cell lysate centrifuged and filtered. ALKBH3 was then purified from the resulting supernatant using Ni affinity chromatography (GE healthcare). with elution achieved by application of gradient to 500 mM imidazole. Further purification was achieved by gel filtration using a HiLoad superdex 75 16/60 (GE healthcare) in a buffer of 25 mM Sodium Phosphate buffer, pH 8.0 containing 150 mM NaCl, 5% (v/v) glycerol and 5 mM β-ME.

***E coli* AlkB expression and purification**

E coli AlkB (encompassing residues 12-216) was expressed and purified as previously reported, with modifications.[8,10,11] BL21 (DE3) Rosetta T1R cells transformed with pNIC28-Bsa4 ΔN11 AlkB were grown in a LEX system using 750 mL of Terrific Broth (TB) supplemented with 8 g/L of glycerol and appropriate antibiotics. The culture was incubated at 37 ^{o}C in the LEX system with aeration and agitation through the bubbling of filtered air through the culture. When the OD_{600} reached ~2, the temperature was reduced to 18 ^{o}C and the cultures were induced after 30 to 60 min by addition of 0.5 mM IPTG. Growth was continued for 16-20 h and harvested by centrifugation. The cell pellets were resuspended in 1.5 times the cell pellet weight of lysis buffer containing 100 mM HEPES, 500 mM NaCl, 10 mM Imidazole, 10% glycerol, 0.5 mM TCEP, pH 8.0, Benzonase (4 uL per 750 mL cultivation) 250 U/uL from Merck, Protease Inhibitor Cocktail Set III, EDTA free (1000x dilution in lysis buffer) from Calbiochem and stored at -80^{0}C. Cells were lysed on ice by sonication, and the lysate cleared by centrifugation and filtration. Filtered lysates were loaded onto 1 mL Ni-NTA Superflow (Qiagen) in IMAC Wash buffer 1 (20 mM HEPES, 500 mM NaCl, 10 mM imidazole, 10 % (v/v) glycerol, 0.5 mM TCEP, pH 7.5) and subsequently washed with IMAC Wash buffer 2 (20 mM HEPES, pH7.5, 500 mM NaCl, 25 mM imidazole, 10% (v/v) glycerol, 0.5 mM TCEP). Bound proteins were eluted with 500 mM imidazole and loaded onto a HiLoad 16/60 Superdex-200 column (GE Healthcare) pre-equilibrated with 20 mM HEPES, pH 7.5, 300 mM, NaCl, 10% (v/v) glycerol, 0.5 mM TCEP. $AlkB_{12-216}$ has previously been shown to be catalytically active.[8]

Human FTO expression and purification

Full length human FTO was expressed and purified as previously reported, with modifications.[8,12] Full length human FTO was sub-cloned into pNIC28-Bsa4 to generate a His_6-tagged FTO_{1-505} construct, which was transformed into *E. coli* BL21 (DE3) Rosetta cells. The transformed cells were grown at 37 °C and 200 rpm until an OD_{600} of 0.6 was reached. FTO expression was then induced with 0.5 mM isopropyl β-D-1-thiogalactopyranoside (IPTG, Gold Biotechnology). Cell growth was continued at 16 °C for 16 h, after which the cells were harvested by centrifugation and the resulting cell pellet was stored at -80 °C. The frozen cell pellets were thawed and re-suspended to homogeneity in 25 mM Tris buffer (pH 7.5) containing 500 mM NaCl, 40 mM imidazole and 5 mM β-mercaptoethanol (β-ME). The cells were then disrupted by sonication on ice, and the cell lysate centrifuged and filtered. FTO was then purified from the resulting supernatant using Ni affinity chromatography (GE healthcare). Further purification of FTO was achieved by gel filtration using a HiLoad superdex 200 26/60 (GE healthcare) in a 25 mM Tris buffer (pH 7.5) containing 100 mM NaCl, 5% (v/v) glycerol and 5 mM β-ME.

Human ALKBH5 expression and purification

Human ALKBH5 (encompassing residues 66-292) was expressed and purified as previously reported, with modifications.[8,12] A His_6-tagged $ALKBH5_{66-292}$ construct in pNIC28-Bsa4a was transformed into *E. coli* BL21 (DE3) Rosetta cells. The transformed cells were grown at 37 ^oC and 200 rpm to an OD_{600} of 0.6. Protein expression was induced by addition of 0.5 mM IPTG (Gold Biotechnology). Growth was continued at 16 ^oC for 16 h, after which the cells were harvested by centrifugation. The resulting cell pellet was stored at -80 ^oC. Cell pellets were resuspended to homogeneity in 20 mM Tris, pH 8.0, 500 mM NaCl, 40 mM imidazole, pH 8.0 and 5 mM β-ME. The cells were then disrupted by sonication on ice, and the cell lysate centrifuged and filtered. ALKBH5 was purified from the crude cell lysate by Ni affinity chromatography (GE healthcare), with elution achieved by application of gradient to 500 mM imidazole. This was followed by anion chromatography using a 5 mL HiTrap Q HP column (GE healthcare), with elution achieved by application of gradient to 1 M NaCl. Further purification was achieved by gel filtration using a HiLoad superdex 75 26/60 (GE healthcare) in a buffer of 20 mM Tris, pH 8.0, 100 mM NaCl and 5 mM β-ME. $ALKBH5_{66-292}$ has previously been shown to be catalytically active.[8]

Conformational probe-DSF demethylase assay

The assay was performed in triplicate in a final reaction volume of 50 µL. Reaction consisted of the enzyme (50 nM), m^1A-probe (substrate; 10 µM), 2-oxoglutarate (10 µM), $(NH_4)_2Fe(SO_4)_2 \cdot 6H_2O$ (10 µM), and L-ascorbate (200 µM) in 50 mM HEPES buffer, pH 7.0. The reaction was incubated at 4 ºC for the specified time points (see Figure S6, Supplementary Information), after which SYBR Green I (20x; Invitrogen) was added, and the reaction mixture was analysed on a CFX96 Real-Time PCR Detection System (Bio-Rad). Melting curve was obtained by steady heating from 25 °C to 95 °C at a rate of 1 °C / min^{-1}. Fluorescence were detected on FAM channel, with readings taken every 0.5 °C. The software provided was then used to obtain the negative first derivative plots and the T_m values. The concentrations of the demethylated product was determined based on their T_m values, using calibration plots obtained from pure demethylated products shown below. Controls without enzyme were also set up. The percentage of demethylation was then obtained using the calculated concentrations.

IC_{50} determination. Eight different concentrations of inhibitors were used (0, 1, 3, 10, 30, 100, 300, 1000 µM); the IC_{50s} were then calculated from the variation in percentage demethylation at different inhibitor concentrations, using nonlinear regression, with normalized dose-response fit on GraphPad Prism 6.0™. The assay was performed in triplicate for each inhibitor.

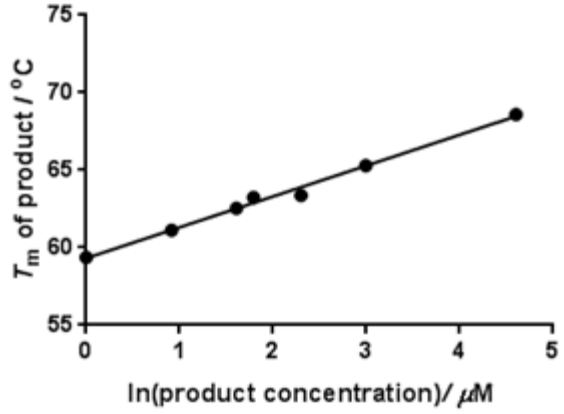

Y = 1.990*X + 59.32

HPLC-based demethylase assay

The assay was modified from previously reported method.[8] The assay was performed in triplicate in a final reaction volume of 25 µL. Reaction consisted of the enzyme (0.1 µM), m^1A-probe or m^1A-ssRNA (5'-AAAGCAG(m^1A)AUUCGAA-3') (10 µM), 2-oxoglutarate (150 µM), $(NH_4)_2Fe(SO_4)_2 \cdot 6H_2O$ (150 µM), and L-ascorbate (2 mM) in 50 mM HEPES buffer, pH

7.0. The reaction was incubated at 4 ºC for the specified time points (see Figure S3, Supplementary Information), before analysis on a bio-inert HPLC system. The m^1A-probe substrate and the corresponding demethylated product were separated using a Dionex DNAPac PA200 anion-exchange column (8 µm, 4 mm × 25 mm) with a gradient of 98% solvent A (50 mM sodium citrate buffer, pH 5.3) to 35% solvent B (50 mM sodium citrate buffer, pH 5.3 with 1.0 M sodium chloride) over 10 min, at a flow rate of 1 mL/min at 40 °C. The UV detection wavelength was set at 266 nm. Controls without enzyme were also set up. The percentage demethylation was estimated based on the peak areas of the m^1A-probe relative to the control.

For IC_{50} determination, eight different concentrations of inhibitors were used (0, 1, 3, 10, 30, 100, 300, 1000 µM); the IC_{50s} were then calculated from the variation in percentage demethylation at different inhibitor concentrations, using nonlinear regression, with normalized dose-response fit on GraphPad Prism 6.0™. The assay was performed in triplicate for each inhibitor in a final reaction volume of 25 µL.

Steady-state kinetic analyses of the demethylation of m^1A-probe, m^1A-containing ssRNA and dsRNA.

The substrates investigated include m^1A-probe, m^1A-containing ssRNA r(AAAGCAG**m^1A**AUUCGAA) and m^1A-containing dsRNA r(AAAGCAG**m^1A**AAUUCGAA) / r(UUCGAAUUCUGCUUU). The K_m and k_{cat} values of ALKBH2, ALKBH3 and AlkB were determined by keeping a constant enzyme concentration of 50 nM and varying the substrate concentrations (2.5, 5, 10, 15, 20 and 30 µM). The concentration of demethylated product at different substrate concentrations was plotted as a function of time (see Figure S4 and S5, Supplementary Information). The initial velocity (V_0) for each substrate concentration was determined from the slope of the curve at the beginning of a reaction. The Michaelis–Menten curve was fitted using non-linear regression, and the kinetic constants (V_{max}, K_m) of the substrate was estimated using GraphPad Prism. All reactions were performed at 4 ºC in triplicate and were adjusted to ensure that less than 20% of the substrate was consumed.

References

(1) Mikhailov, S. N.; Rozenski, R.; Efimtseva, E. V.; Busson, R.; Aerschot, A. V. and Herdewijn, P. *Nucleic Acids Res.* **2002**, 30, 1124–1131.

(2) Engel, J. D. *Biochem. Biophys. Res. Commun.* **1975**, 64, 581-586.

(3) Marky, L. and Breslauer, K. *Biopolymers* **1987**, 26, 1601–1620.

(4) Xia, T.; Mathews, D. H. and Turner, D. H. (1999) Thermodynamics of RNA secondary structure formation. In Söll, D.; Nishimura, S. and Moore, P. (eds), *Comprehensive Natural Product Chemistry*. Elsevier, Oxford, UK, Vol. 8, pp. 21–47.

(5) Piotto, M.; Saudek, V. and Sklenar, V. *J. Biomol. NMR* **1992**, 2, 661–665.

(6) Yang, C. G.; Yi, C.; Duguid, E. M.; Sullivan, C. T.; Jian, X.; Rice, P. A. and He, C. *Nature* **2008**, 452, 961-965.

(7) Duncan, T.; Trewick, S. C.; Koivisto, P.; Bates, P. A.; Lindahl, T. and Sedgwick, B. *Proc. Natl. Acad. Sci. U.S.A.* **2002**, 99, 16660-16665.

(8) Toh, J. D. W.; Sun, L.; Lau, L. Z. M.; Tan, J.; Low, J. J. A.; Tang, C. W. Q.; Cheong, E. J. Y.; Tan, M. J. H.; Chen, Y.; Hong, W.; Gao, Y. G. and Woon, E. C. Y. *Chem. Sci.* **2015**, 6, 112-122.

(9) Aas, P. A.; Otterlei, M.; Falnes, P. O.; Vagbo, C. B.; Skorpen, F.; Akbari, M.; Sundheim, O.; Bjoras, M.; Slupphaug, G.; Seeberg, E. and Krokan, H. E. *Nature* **2003**, 421: 859-863.

(10) Woon, E. C. Y.; Demetriades, M.; Bagg, E. A.; Aik, W.; Krylova, S. M.; Ma, J. H.; Chan, M.; Walport, L. J.; Wegman, D. W.; Dack, K. N.; McDonough, M. A.; Krylov, S. N. and Schofield, C. J. *J. Med. Chem.* **2012**, 55, 2173-2184.

(11) Savitsky, P.; Bray, J.; Cooper, C. D.; Marsden, B. D.; Mahajan, P.; Burgess-Brown, N. A. and Gileadi, O. *J. Struct. Biol.* **2010**, 172, 3-13.

(12) Han, Z.; Niu, T.; Chang, J.; Lei, X.; Zhao, M.; Wang, Q.; Cheng, W.; Wang, J.; Feng, Y. and Chai, J. *Nature* **2010**, 464, 1205-1209.

(13) Aik, W.; Scotti, J. S.; Choi, H.; Gong, L.; Demetriades, M.; Schofield, C. J. and McDonough, M. A. *Nucleic Acids Res.* **2014**, 42, 4741-4754.

Author contributions

The study was designed by Esther C. Y. Woon.

Syntheses and characterizations of all compounds were carried out by Tianming Yang.

Protein expression and purifications were carried out by Tianming Yang and Shui Zou.

Biochemical assays, DSF-based melting analyses, and kinetic analyses were carried out by Adeline Cheong and Xiangrui Mai.

The manuscript was written by Esther C. Y. Woon, with assistance and comments from all other authors.

The authors declared no competing financial interests.